Reduction of Nonspecific Binding for Cellular Imaging Using Quantum Dots Conjugated with Vitamin E

Jie Pan, Dong Wan, Yuxia Bian, and Yugao Guo
State Key Laboratory of Hollow Fiber Membrane Materials and Processes, School of Environmental and Chemical Engineering, Tianjin Polytechnic University, Tianjin 300387, China

Fengmin Jin, Tuo Wang, and Jinlong Gong
Key Laboratory for Green Chemical Technology of Ministry of Education, School of Chemical Engineering and Technology, Tianjin University, Tianjin 300072, China

Collaborative Innovation Center of Chemical Science and Engineering, Tianjin 300072, China

DOI 10.1002/aic.14382
Published online February 12, 2014 in Wiley Online Library (wileyonlinelibrary.com)

Quantum dots (QDs) as luminescence probes play an important role in the field of life sciences and medicine in recent decades. However, hydrophobic QDs have many limitations in applications for biological imaging such as insolubility in aqueous solutions and nonspecific binding to cellular membranes and so on. This article describes the design and synthesis of D-α-tocopheryl polyethylene glycol 3350 succinate ($TPGS_{3350}$)-conjugated QDs ($TPGS_{3350}$-QDs) nanoparticles (NPs) for effective reduction of nonspecific cellular binding of QDs for biological imaging. $TPGS_{3350}$ with n-poly(ethylene glycol) $(PEG)_{3350}$ group was used in order to enhance the stabilization and water solubility of QDs, and reduce nonspecific cellular binding of NPs with the function of long-chain PEG_{3350}. We have demonstrated that $TPGS_{3350}$-QDs NPs show good stability and dispersion in aqueous solutions and that small amount of $TPGS_{3350}$-QDs NPs were nonspecific bound with Michigan Cancer Foundation-7 (MCF-7) cells in comparison of mercaptoacetic acid-coated QDs NPs, which confirmed $TPGS_{3350}$ can efficiently reduce nonspecific cellular binding due to the effect of PEG_{3350} in $TPGS_{3350}$. The nonspecific binding of $TPGS_{3350}$-QDs NPs was also found to be much lower than that of TPGS-QDs NPs. The developed $TPGS_{3350}$-QDs NPs in this study could be a promising tool for molecular imaging such as in vivo cell trafficking studies.
 AIChE J, 60: 1591–1597, 2014
Keywords: quantum dots, cellular imaging, nanoparticles, nonspecific cellular binding, cancer nanotechnology

Introduction

Fluorescence techniques are important tools in the field of life sciences. Many biological applications including cellular and molecular imaging, cell labeling and tracking, multiplexed analyses, and DNA detection make use of fluorescence techniques. The biocompatible, reliable fluorescent marker with good photophysical properties will be an ideal fluorescent reporter for the broad applicability of fluorescence techniques.[1–6] Fluorescent proteins[7] and organic dyes[8] have small size and good biocompatibility, which is helpful for their applications for labeling cells and subcellular targets. But their poor photostability limits their applicability. Quantum dots (QDs) as luminescence probes received extensive attentions in various fields such as life and medicine in recent decades. Compared with the conventional dyes, QDs have many improved optical qualities desirable for biological applications such as tunable emission from visible to infrared wavelengths by changing their size and composition, broader excitation spectra due to high absorption coefficients, high quantum yield of fluorescence, strong brightness, photostability, and high resistance to photobleaching, which are advantageous for QDs widely used in biomedical labeling, molecule tracking, and imaging.[9–15] But QDs are utilized successfully in biological applications to face various critical challenges such as their water solubility, colloidal stability, and nonspecific cellular binding.[16,17]

Two ways including surface ligand exchange and amphiphilic polymer coatings have been developed to render QDs soluble in aqueous solutions in recent years.[11,14,18] For ligand exchange, the ligand of QDs' surface can be exchanged with thiol-containing molecules with a hydrophilic end. For example, mercaptoacetic acid (MAA) was exchanged to QDs, in which mercapto group binds to Zn atom, and the carboxylic group enabled the QDs soluble in aqueous solutions.[15] For amphiphilic polymer coatings, QDs were coated with a layer of amphiphilic molecules, which contain hydrophilic and hydrophobic moieties. Gao et al. developed QDs coated with ABC triblock copolymer linking with tumor-targeting ligands for *in vivo* cancer imaging.[19] Additionally, Sukhanova et al. fabricated biocompatible QDs with high bright (photoluminescence (PL) quantum yield >60%) through formulating a double-layered solubilizing

Jie Pan and Dong Wan contributed equally to this work.

Correspondence concerning this article should be addressed to J. Gong at jlgong@tju.edu.cn.

shell on the surface of QDs.[20] Moreover, QDs can be formulated in an amphiphilic polymer shell by nonspecific hydrophobic interaction between the alkyl chains of poly (maleic anhydride alt-1-tetradecene) and the QDs surfactant molecules.[21] Furthermore, QDs can also be encapsulated in phospholipid micelles of a mixture of *n*-poly(ethylene glycol) phosphatidylethanolamine (PEG)and phosphatidylcholine.[22] Pan and Feng prepared QDs-loaded nanoparticles of biodegradable polymers with folate decoration for targeted cellular imaging.[23] These NPs improved imaging specificity and sensitivity of QDs. Our group also synthesized PEGylated liposome coated QDs/mesoporous silica core-shell NPs for cellular imaging, which used low toxicity and immunogenicity of liposome structure combined with the wide range of photochemical characteristics of the QDs/mesoporous silica core-shell NPs.[24]

Moreover, QDs must also be efficient fluorescence, colloidal stability, and especially low nonspecific cellular binding for efficient biological applications. Nonspecific cellular binding is a major challenge in bioimaging.[25,26] Generally, QDs can nonspecifically bind onto the cell membranes, proteins, which lead to high level of background fluorescence, and reduce the sensitivity of imaging. To address the nonspecific binding of QDs, different approaches were exploited in recent years. The developed hydroxyl-coated QDs by Nie and coworkers significantly reduced nonspecific binding compared to those functionalized with carboxylate and streptavidin.[26] Furthermore, PEG is hydrophilic and biocompatible, and is often linked to the surfaces of nanoparticles for improving water solubilization and reduction of nonspecific binding, which helps the NPs escape from being recognized and eliminated by the reticuloendothelial system.[27] Many studies indicated that PEG-modified QDs can significantly reduce nonspecific cellular binding.[25,28–32]

D-α-Tocopheryl polyethylene glycol 1000 succinate (TPGS) is a water-soluble derivative of natural vitamin E, which has amphiphilic structure comprising lipophilic alkyl tail and hydrophilic polar head portion. TPGS is an excellent emulsifier, solubilizer, and bioavailability enhancer of hydrophobic agents due to its bulky structure and large surface area. Furthermore, TPGS contains PEG_{1000} groups, which are particularly effective steric stabilizers to protect nanoparticles from opsonization and phagocytocis, and improve the aqueous solubility of nanoparticles.[23,33–36] Unfortunately, although TPGS contains PEG_{1000} groups, Feng and coworkers reported that the chain length of PEG_{1000} in TPGS is short for decreasing nonspecific adsorption.[37] Consequently, Feng and coworkers prepared $TPGS_{2000}$ using PEG_{2000} to improve successfully the stability of NPs and reduce nonspecific binding of NPs with the function of long-chain PEG_{2000} surfaces.[37] Furthermore, it was described by Bentzen et al. that the length of PEG chain can effect on the nonspecific binding.[25] They pointed out that nonspecific binding of PEG-coated QDs to Human Embryonic Kidney (HEK) cells increased with decreasing PEG length. Here, $TPGS_{3350}$ containing PEG_{3350} were developed to be conjugated with QDs. Such $TPGS_{3350}$ on the surface of QDs should ensure aqueous solubilization, colloidal stability, and weak nonspecific interaction of QDs with cells.

In this study, D-α-tocopheryl polyethylene glycol 3350 succinate (Vitamin E $TPGS_{3350}$)-conjugated QDs NPs ($TPGS_{3350}$-QDs NPs) were developed. Hydrophobic QDs were first treated with MAA to obtain MAA-coated QDs. Next, MAA-coated QDs were reacted with amine-terminated $TPGS_{3350}$ ($TPGS_{3350}$-NH_2) via 1-ethyl-3-(3-dimethylaminopropyl)carbodiimide (EDC)/*N*-hydroxysuccinimide (NHS) method to prepare $TPGS_{3350}$-QDs NPs. It was found in this study that the developed $TPGS_{3350}$-QDs NPs exhibit good colloidal stability, high quantum yields, and pronounced reduction of nonspecific cellular binding.

Materials and Methods

Materials

TOPO coated CdSe/ZnS core/shell QDs were synthesized according to literature procedures.[38] The calculation of QDs concentration was described by Ballou et al.[39] QD concentration was determined by absorbance using appropriate extinction coefficients. MAA, D-α-tocopherol succinate (α-TOS), D-a-tocopheryl polyethylene glycol 1000 succinate (TPGS), polyoxyethylene bis(amine) (MW 3350), *N*,*N*′-dicyclohexylcarbodiimide (DCC), 4-dimethylaminopyridine (DMAP), NHS, dichloromethane (DCM), phosphate buffered saline (PBS), Dulbecco's Modified Eagle's Medium (DMEM) medium, antibiotics (penicillin–streptomycin solution) were from Sigma–Aldrich (St. Louis, MO). Fetal bovine serum (FBS) was purchased from Gibco (Life Technologies, AG, Switzerland). MCF-7 breast cancer cells were provided by American Type Culture Collection. Millipore water was produced by the Milli-Q Plus System (Millipore Corporation, Bedford).

Preparation of $TPGS_{3350}$-QDs NPs

MAA-coated QDs were made by the protocol described in the literature.[40] This procedure renders QDs aqueous solubilization with carboxyl-terminated surface functional groups, which is used to facilitate $TPGS_{3350}$-NH_2 conjugation on the NPs surface. Briefly, QDs were dissolved in chloroform. Furthermore, excess MAA was reacted with colloidal QDs in chloroform for about 2 h. Next, PBS solution was added into this reaction mixture. Finally, MAA-coated QDs in an aqueous solution can be obtained after vigorous shaking and extracting.

D-α-Tocopheryl amino polyethylene glycol 3350 succinate ($TPGS_{3350}$-NH_2) was fabricated following the method reported by Feng and coworkers.[37] In brief, α-TOS was reacted with PEG_{3350} bis-amine through DCC/NHS overnight in nitrogen environment at dark. The stoichiometric ratio α-TOS, PEG_{3350} bis-amine, DCC, and NHS is 1:1.2:2:2. Next, amine-terminated $TPGS_{3350}$ powder can be obtained though filtering, precipitated in cold diethyl ether and freeze drying.

MAA-coated QDs (2 mL of 1 mM QDs) was dissolved in borate buffer at pH 8.4 and then activated with EDC and NHS (with a molar ratio of MAA-coated QDs /EDC/NHS equivalent to 1:1:2.5) at room temperature for 1 h. $TPGS_{3350}$-NH_2 dissolved in 10 mL DMSO were added to the activated MAA-coated QDs solution, and the mixture was stirred gently for 2 h at room temperature in dark. The $TPGS_{3350}$-QDs NPs were purified by centrifugation at 10,000 rpm for 15 min and washed 3–4 times with 0.01 M PBS (pH 7.4).

For evaluation the effect of chain length of PEG in TPGS on nonspecific binding QDs to cells, TPGS-QDs NPs were also synthesized in this study. The approach of TPGS-QDs NPs was similar to the procedure of preparing $TPGS_{3350}$-QDs NPs excepting to use TPGS-NH_2, which can be fabricated as following: 0.5 mM TPGS was activated at 100°C

under nitrogen atmosphere for 24 h by 1 mM succinic anhydride in the presence of 1 mM DMAP. Next, the product was dissolved in DCM and then precipitated in cold methanol. Furthermore, the activated 0.12 mM TPGS was reacted with 0.12 mM ethylene diamine in the presence of 0.36 mM DCC and 0.36 mM NHS in DMSO at room temperature under nitrogen atmosphere for 24 h. The product was filtered to remove *N*,*N*-dicyclohexylurea and then dialyzed using MWCO 1000 membrane in DMSO for 24 h to remove excess reagents, and further dialyzed against Millipore water for 24 h to remove DMSO.

Characterization of $TPGS_{3350}$-QDs NPs

Average particle-size and size distribution of the NPs were measured with laser light scattering (LLS, 90 Plus Particle Size, Brookhaven Instruments Co.) at a laser angle of 90° at 25°C. NPs were dropped into deionized water and sonicated for 1 min in order to ensure homogenous dispersion of the particles. The surface charge of the $TPGS_{3350}$-QDs NPs in water was determined using ZetaPlus zeta potential analyzer (Brookhaven Instruments Corporation) at 25°C. Transmission electron microscope (TEM, JEM-2010F, JEOL, Japan) were exploited to investigate morphology of NPs. NPs suspension was dropped on the surface of copper grid with carbon film and dried at room temperature. Surface chemistry of $TPGS_{3350}$-QDs NPs was analyzed by x-ray photoelectron spectroscopy (XPS) with an Al Kα x-ray source (1486.6 eV photons) (XPS, AXIS His-165 Ultra, Kratos Analytical, Shimadzu Corporation, Japan). A binding energy (BE) ranged from 0 to 1100 eV was recorded in the survey spectrum with pass energy of 80 eV under the fixed transmission mode. The fluorescence quantum yield (QY) of the QDs in deionized water were measured using Rhodamine 6G as fluorescence standard.[41] The fluorescent image of $TPGS_{3350}$-QDs NPs was recorded with a digital color camera (EOS 400D, Canon, Japan). Briefly, 1 mL of the sample was placed in quartz cuvettes. The fluorescent image of the NPs suspension in water was recorded with a digital color camera under the radiation of UV lamp with excitation wavelength at 365 nm (Model UVGL-58, CA). The emission spectra of the NPs aqueous suspension placed into a quartz cuvette was measured using a spectroflurophotometer (RF-5301PC, SHIMADZU, Japan) at excitation 405 nm.

Study of nonspecific binding of NPs to cells

Cell *Cultures*. MCF-7 human breast adenocarcinoma cells were used to carry out cell line experiments. Cells were cultured in the DMEM supplemented with 10% FBS and 1% penicillin–streptomycin as the antibiotics in humidified environment of 5% CO_2 at 37°C. Growth medium was replenished every other day and subculture was performed when cells reached 80% confluence.

Qualitative Study of Nonspecific Binding of NPs to Cells. For qualitative study of nonspecific binding, MCF-7 cells were cultured in chamber (LAB-TEK, Chambered Coverglass System) at 37°C. After 80% confluence, the medium was removed, and the adherent cells were washed twice with a 1× PBS buffer. Next, MAA-coated QDs NPs, TPGS-QDs NPs, and $TPGS_{3350}$-QDs NPs at 1-nM QDs concentration in the medium were added into the chamber. After incubation for 4 h to allow the cells to internalize the NPs, the cells were rinsed 3 times with 1× PBS buffer. Furthermore, cells were fixed with 75% ethanol about 20 min, and then the nuclei of the cells were stained with 4′,6-diamidino-2-phenylindole dihydrochloride (DAPI) about 30 min. The cells were washed twice again with 1× PBS buffer and imaged with a confocal laser scanning microscope (CLSM, Zeiss LSM 410, Germany) with imaging software (Fluoview FV1000). The images of NPs and the nuclei of the cells stained by DAPI were recorded with following channels: blue channel (DAPI) with excitation at 340 nm and red channel (QDs) with excitation at 405 nm.

Quantitative Study of Nonspecific Binding of NPs to Cells. For quantitative analysis of nonspecific binding NPs to cells, MCF-7 cells were seeded into 96-well black plates (Costar, IL) at 1×10^4 cells/well. After the cells reached 80% confluence, the medium was replaced with the suspension of $TPGS_{3350}$-QDs NPs, TPGS-QDs NPs, and MAA-coated QDs NPs in DMEM medium at the concentration of 2-nM QDs. Six wells for positive control and six wells for sampling were seeded for each sample. After incubation for 2 or 4 h, suspensions of the NPs were removed and the wells were washed with 50 μL of 1× PBS for 3 times to remove traces of NPs. Next, after 100 μL of fresh medium was then added to each sample well, 50 μL of 0.5% Triton X-100 in 0.2 N NaOH was added to lyse the cells. The fluorescence intensities of each well at 650 nm were recorded with a microplate reader (Genios, Tecan, Männedorf, Switzerland) with excitation wavelength at 405 nm. The nonspecific cellular binding efficiency was calculated as the ratio of the fluorescence in the sample wells to that of the positive control.

Results and Discussion

Preparation of $TPGS_{3350}$-QDs NPs

To reduce nonspecific binding in live cell assays, $TPGS_{3350}$ was conjugated to the surface of the QDs. The schematic illustration of fabricating $TPGS_{3350}$-QDs NPs is shown in Figure 1. First, the phase transfer of QDs is accomplished through ligand exchange with MAA. Organic QDs in chloroform were added into the MAA solution to stir about 2 h, followed by PBS solution added into this reaction mixture under vigorous shaking and extracting. Thus, MAA-coated QDs in an aqueous solution can be obtained. The mercapto group of MAA binds to a Zn atom in QDs, whereas the carboxylic acid group of MAA make the QDs dissolve in aqueous buffers, and also the carboxyl group on the MAA-coated QDs can be used to further surface modification. $TPGS_{3350}$-NH_2 with amine group can be conjugated to the surface of MAA-coated QDs via EDC/NHS at borate buffer at pH 8.4. It was reported that etching of the surface of QDs by HCl from EDC hydrolysis does not reduce fluorescence from QDs as the borate buffer maintained a pH of 8.5–8.2 throughout reaction.[25] In order to decrease nonspecific binding of QDs, the surface of QDs could be modified by $TPGS_{3350}$ containing PEG_{3350}, which can reduce the electrostatic interactions of QDs with the surface of the cell or proteins expressed in the extra cellular matrix. Further, PEG_{3350} on the surface of QDs can change the electrical double layer surrounding of QDs, which can be helpful to further reduce nonspecific binding. The conjugation of $TPGS_{3350}$ on the surface of QDs could also render water soluble and good colloidal stability of QDs.

Characterization of NPs

Dynamic light scattering (DLS) was utilized to determine the size and size distribution of the $TPGS_{3350}$-QDs NPs. The

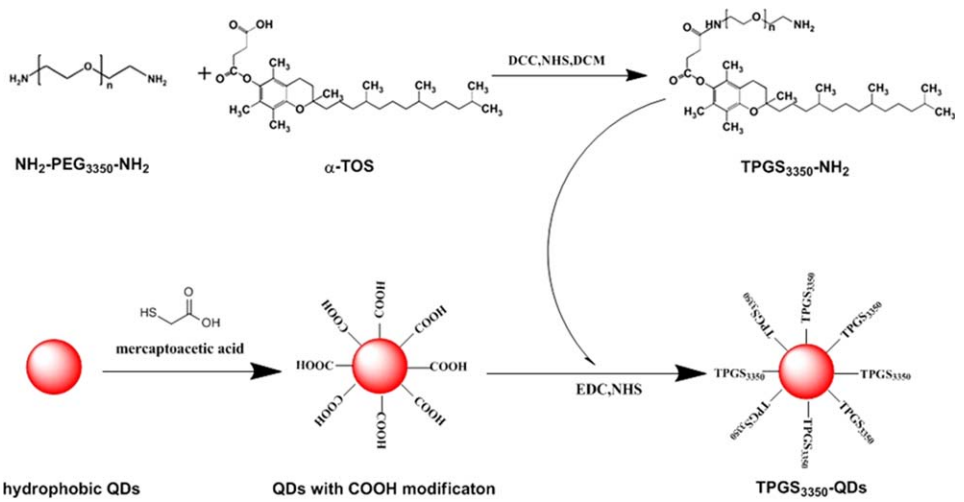

Figure 1. The scheme of preparation of $TPGS_{3350}$-QDs NPs.

[Color figure can be viewed in the online issue, which is available at wileyonlinelibrary.com.]

mean hydrodynamic size and polydispersity index of $TPGS_{3350}$-QDs NPs was measured to be 8.1 ± 0.3 nm and 0.102 ± 0.004, respectively. QDs with small sizes are promising tools for cell labeling applications, because the small size reduces the possibility of the probe interfering with receptor function, and renders more QDs to reach hindered regions such as synapse. Furthermore, it was found that there is no significant change in $TPGS_{3350}$-QDs NPs size or size distribution after storing the NPs at 4°C for 1 month. This result confirms that the $TPGS_{3350}$-QDs NPs have high stability in aqueous solutions. The zeta potential of $TPGS_{3350}$-QDs NPs was found to be -21.6 ± 0.2 mV, which is important to maintain the stability of the NPs suspension due to the strong repellent forces among particles. Moreover, the value of zeta potential is an important parameter for nonspecific cell binding, which is partly due to electrostatic interactions of the cell surface with charged QD ligand coatings. The zeta potential of $TPGS_{3350}$-QDs NPs developed in this study is beneficial to hinder this electrostatic interaction between cells with QDs. The morphology of the NPs was observed by TEM. As shown in Figure 2B, $TPGS_{3350}$-QDs NPs appeared spherical and well-dispersed on the copper mesh after drying from water. But it could be found in Figure 2A that original hydrophobic QDs were aggregated. This result illustrated that the modification of $TPGS_{3350}$ can enhance the dispersion of QDs in solution, which is important for cell labeling and single-particle tracking applications. Moreover, it can be noticed in Figure 2, the size of original QDs is similar as that of $TPGS_{3350}$-QDs NPs, which indicated that the conjugation of $TPGS_{3350}$ to QDs' surface did not effect on sizes of QDs. $TPGS_{3350}$-QDs NPs observed from TEM is about 8.0 nm in size, which coincides with the hydrodynamic diameter of $TPGS_{3350}$-QDs NPs from DLS analysis.

The surface chemistry of the NPs was observed by XPS. Figure 3 shows the XPS C1s, N1s, and S2p core-level spectra of $TPGS_{3350}$-QDs NPs. The C1s peak components with BEs at about 284.6, 285.6, 286.2, 287.6, and 288.3 eV is attributable to C—C or C—H, C—N, C—O, O=C—NH, and O=C—O species, respectively. The N1s core-level spectra with BE at about 399.4 eV are attributable to the amine group, linking the MAA-coated QDs, and $TPGS_{3350}$. The $S2p^{3/2}$ and $S2p^{1/2}$ spin-orbit split doublet with BEs at about 162 and 163.2 eV are attributable to the bound sulfur of MAA on the QDs surface, indicating chemical interaction between the sulfur head groups in MAA and the QDs surface. The XPS results indicate that $TPGS_{3350}$ has been covalently immobilized on the surface of MAA-coated QDs.

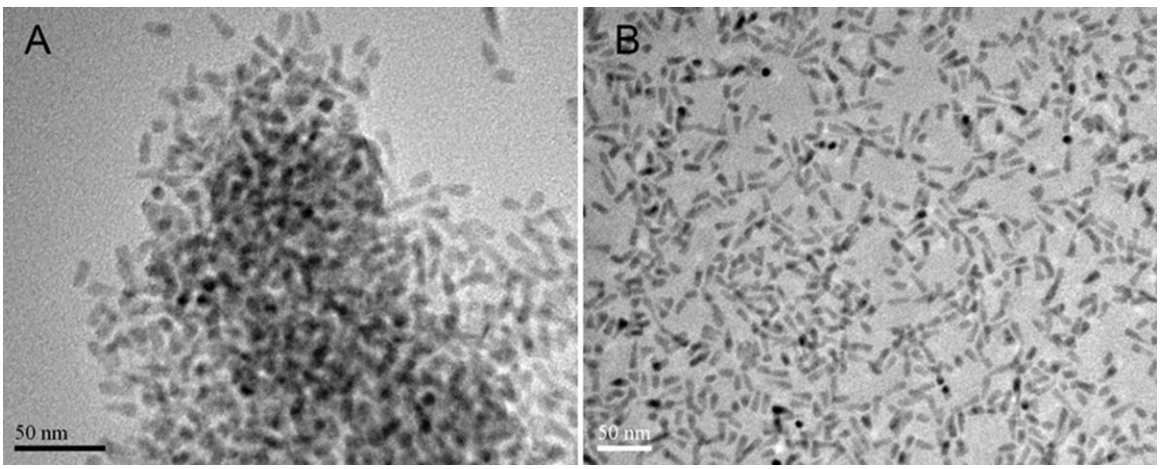

Figure 2. TEM image of (A) original hydrophobic QDs and (B) $TPGS_{3350}$-QDs NPs.

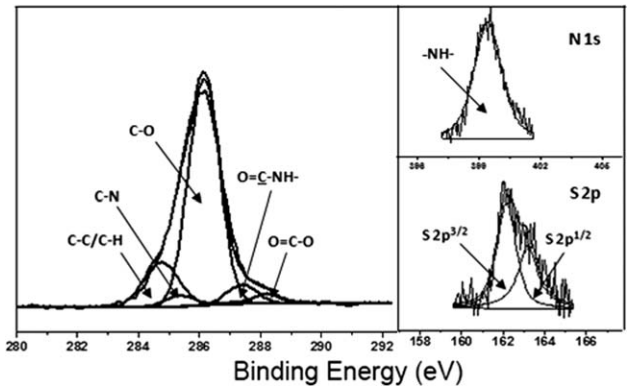

Figure 3. XPS image of C1s, N1s, and S2p core-level spectra of the $TPGS_{3350}$-QDs NPs surface.

The fluorescent image (shown in Figure 4) of $TPGS_{3350}$-QDs NPs dispersed in water was recorded with a digital color camera under UV lamp with excitation wavelength of 365 nm. It could be seen that NPs emitted red fluorescence with a pure color. And also, no aggregation and precipitation of these NPs were found in Figure 4. The emission spectrum of $TPGS_{3350}$-QDs NPs was illustrated in Figure 5. Dispersion of NPs in water demonstrated a symmetrical fluorescence emission spectrum with an emission maximum at 650 nm under excited at 405 nm. These findings prove that $TPGS_{3350}$-QDs NPs display outstanding property of fluorescence. Moreover, the fluorescence QYs were investigated. The findings also demonstrated that QYs of the original hydrophobic QDs in chloroform and the $TPGS_{3350}$-QDs NPs in deionized water are 46 and 40%, respectively.

Nonspecific cellular binding of NPs

The issue of nonspecific cellular binding of NPs is complicated. It was reported that nonspecific cellular binding is

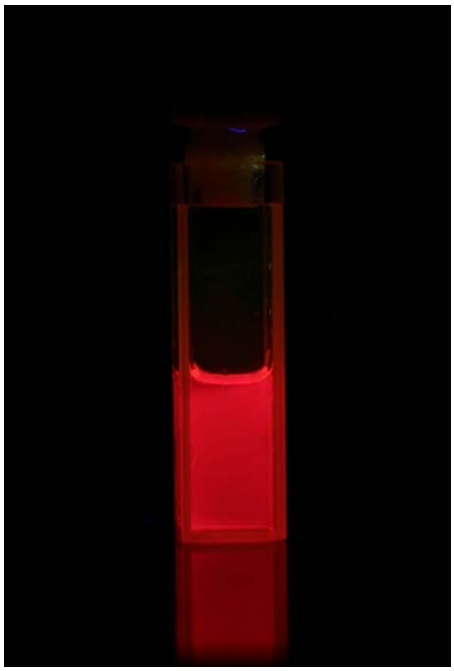

Figure 4. The fluorescent image of $TPGS_{3350}$-QDs NPs dispersed in water under UV lamp with excitation wavelength of 365 nm.

[Color figure can be viewed in the online issue, which is available at wileyonlinelibrary.com.]

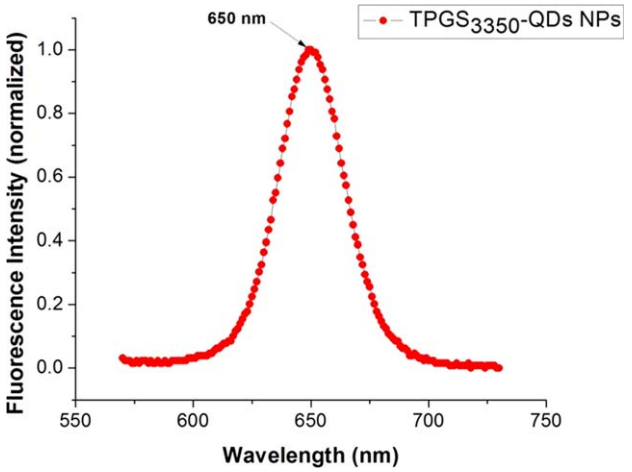

Figure 5. Emission spectrum of $TPGS_{3350}$-QDs NPs in water under 405 nm excitation.

[Color figure can be viewed in the online issue, which is available at wileyonlinelibrary.com.]

associated with hydrophobic interactions between the ligands of NPs and lipids on the cell membranes. Some literatures also described that nonspecific cellular binding is attributed to the electrostatic interactions between the cells and the negatively charged groups on the surfaces of NPs.[25,26] In this study, the qualitative nonspecific cellular binding can be visually verified by the CLSM images. Figure 6 shows CLSM of MCF-7 cells treated with MAA-coated QDs, TPGS-QDs NPs, and $TPGS_{3350}$-QDs NPs at 1-nM QDs concentration at 37°C after 4 h incubation. The images were obtained from (A) the combined red channel and blue channel; (B) the blue channel with excitation at 340 nm; and (C) the red channel with excitation at 405 nm. From Figure 6, it can be observed obviously that red fluorescence emitted from QDs appeared in the cytoplasm around the nuclei (blue, stained by DAPI), which indicated NPs were internalized by MCF-7 cells. Moreover, red fluorescence from MAA-coated QDs NPs in Row 1 is much brighter than that of TPGS-QDs NPs and $TPGS_{3350}$-QDs NPs in Rows 2 and 3. This result indicated nonspecific cellular binding of MAA-coated QDs is obvious, whereas TPGS-QDs NPs or $TPGS_{3350}$-QDs NPs was found to show less nonspecific cellular binding. The explanation for this finding may be due to the effect of PEG group, which can reduce the nonspecific cellular binding, resulting in decreased endocytosis of NPs by cells. Interestingly, as shown in Figure 6, $TPGS_{3350}$-QDs NPs showing excellent reduction of nonspecific binding to cells in comparison with TPGS-QDs NPs. It suggests that $TPGS_{3350}$-QDs NPs have superior performance on reduction of nonspecific cellular binding. This result indicates the chain length of PEG in TPGS is related with the degrees of nonspecific binding of QDs to cells. The results in this study indicated that $TPGS_{3350}$ with long-chain length of PEG_{3350} can efficiently prohibit QDs to be adsorbed on the membranes of cells.

The experiment of quantitative nonspecific cellular binding of NPs by MCF-7 cells was carried out to further evaluate nonspecific cellular binding of NPs. As shown in Figure 7, in contrast for TPGS-QDs NPs and $TPGS_{3350}$-QDs NPs, MAA-coated QDs NPs were used as a control to evaluate the effect of $TPGS_{3350}$ or TPGS on nonspecific cellular binding. After MCF-7 cells incubated for 2 h in DMEM containing $TPGS_{3350}$-QDs NPs and

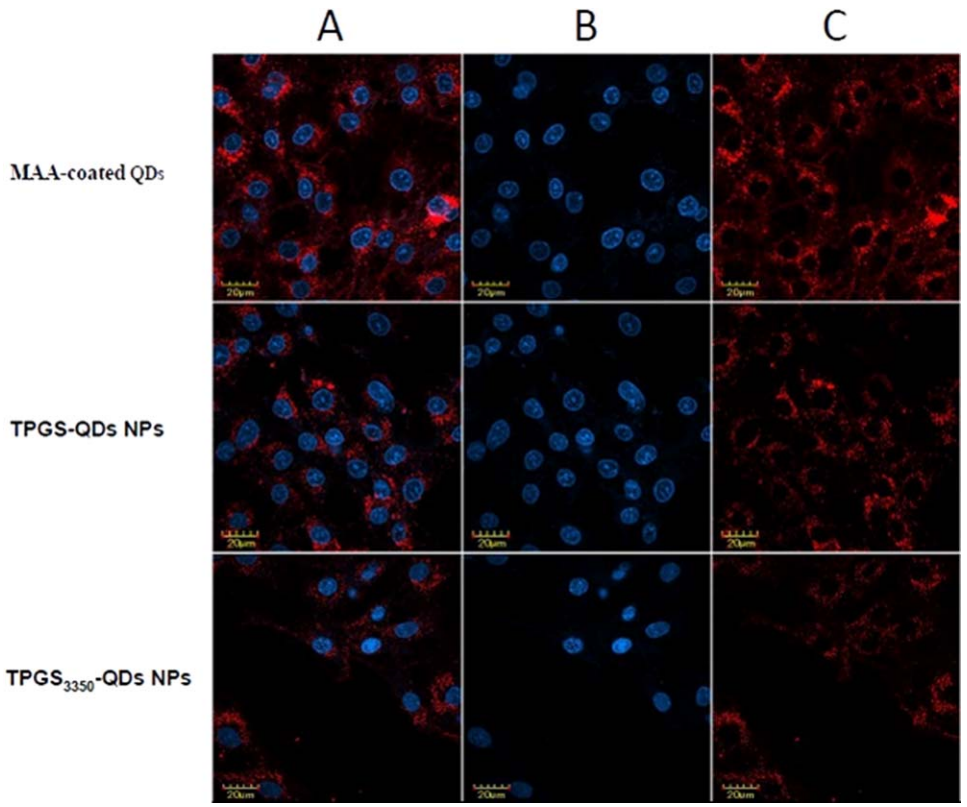

Figure 6. CLSM of MCF-7 cells treated with (Row 1) MAA-coated QDs NPs, (Row 2) TPGS-QDs NPs, and (Row 3) $TPGS_{3350}$-QDs NPs at 1-nM QDs concentration at 37°C after 4 h incubation.

The images were obtained from (A) the combined red channel and blue channel, (B) the blue channel with excitation at 340 nm, and (C) the red channel with excitation at 405 nm. [Color figure can be viewed in the online issue, which is available at wileyonlinelibrary.com.]

MAA-coated QDs NPs at 2-nM QDs, nonspecific cellular binding efficiency of $TPGS_{3350}$-QDs NPs ($10.1 \pm 2.36\%$) is much lower than that of MAA-coated QDs NPs ($22.8 \pm 2.65\%$). Upon 4 h incubation, the nonspecific cellular binding efficiency of $TPGS_{3350}$-QDs NPs was measured to be $11.7 \pm 1.61\%$, which is still low compared to that of MAA-coated QDs ($26.4 \pm 2.53\%$). This phenomenon thus illustrates $TPGS_{3350}$ in NPs can reduce efficiently nonspecific cellular binding of NPs due to PEG_{3350} effect. Furthermore, it can be seen from Figure 7 that TPGS-QDs NPs expressed 1.6- and 1.7-fold higher nonspecific cellular binding than the $TPGS_{3350}$-QDs NPs after 2 and 4 h culture with MCF-7 cells, respectively, which indicate that $TPGS_{3350}$-QDs NPs can achieve low nonspecific cellular binding to cells compared to TPGS-QDs NPs. In this study, it can be found that these results in the experiment of quantitative nonspecific cellular binding consistent with findings measured by CLSM. These results indicate that $TPGS_{3350}$-QDs NPs with minimal nonspecific binding to cells are suitable for cell labeling and single-particle imaging applications.

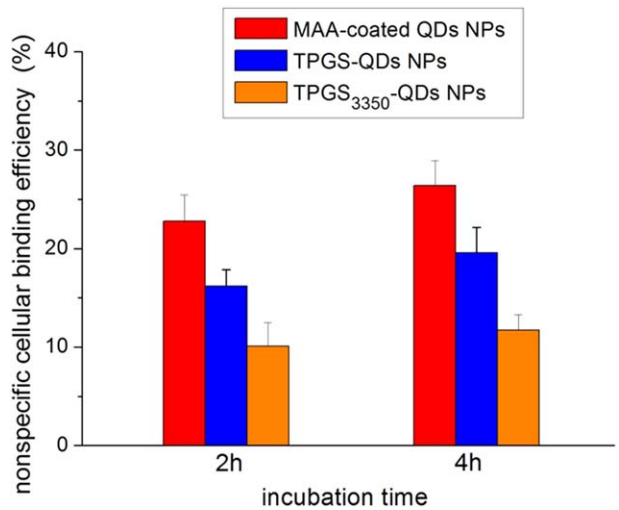

Figure 7. MCF-7 nonspecific cellular binding efficiency of MAA-coated QDs NPs, TPGS-QDs NPs, and $TPGS_{3350}$-QDs NPs in medium at the QDs concentration of 2 nM for 2 and 4.0 h, respectively ($n = 6$).

[Color figure can be viewed in the online issue, which is available at wileyonlinelibrary.com.]

Conclusions

In this study, $TPGS_{3350}$-QDs NPs were fabricated for the reduction of nonspecific cellular binding for cellular imaging. These NPs show excellent colloidal stability with fine hydrodynamic size distribution in aqueous solutions. CLSM imaging demonstrated NPs with red bright fluorescence were localized in the cytoplasm around the nuclei. Additionally, the nonspecific cellular binding of $TPGS_{3350}$-QDs NPs was examined. In contrast with MAA-coated QDs NPs, the $TPGS_{3350}$-QDs NPs showed the reduction of nonspecific cellular binding for MCF-7 cells due to the effect of PEG_{3350} in $TPGS_{3350}$, which indicate that PEG_{3350} in $TPGS_{3350}$ can reduce nonspecific cellular binding of QDs to cells. In

particular, $TPGS_{3350}$-QDs NPs show lower nonspecific cellular binding for MCF-7 cells than TPGS-QDs NPs, which suggest that $TPGS_{3350}$ with long-chain PEG_{3350} in NPs can achieve low nonspecific cellular binding to cells compared with TPGS. The developed $TPGS_{3350}$-QDs NPs with significantly reduced nonspecific cellular binding have valuable applications in bioimaging.

Acknowledgments

Financial support from National Science Foundation of China (20921001, 21172171, 21222604), the 973 program (2011CB933100, 2011CB932402), and Natural Science Foundation of Tianjin (No. 11JCZDJC22300) is acknowledged. The authors are also grateful for financial support from the open funds from the key laboratory of biomedical materials in Tianjin.

Literature Cited

1. Perfézou M, Turner A, Merkoçi A. Cancer detection using nanoparticle-based sensors. *Chem Soc Rev*. 2012;41:2606–2622.
2. Swierczewska M, Liu G, Lee S, Chen X. High-sensitivity nanosensors for biomarker detection. *Chem Soc Rev*. 2012;41:2641–2655.
3. Wang X, Yang L, Cchen Z, Shin DM. Application of nanotechnology in cancer therapy and imaging. *CA Cancer J Clin*. 2008;58:97–110.
4. Ferrari M. Cancer nanotechnology: opportunities and challenges. *Nat Rev Cancer*. 2005;5:161–171.
5. Lang P, Yeow K, Nichols A, Scheer A. Cellular imaging in drug discovery. *Nat Rev Drug Discov*. 2006;5:343–356.
6. Sharrna P, Brown S, Walter G, Santra S, Moudgil B. Nanoparticles for bioimaging. *Adv Colloid Interface Sci*. 2006;123:471–485.
7. Zhang J, Campbell RE, Ting AY, Tsien RY. Creating new fluorescent probes for cell biology. *Nat Rev Mol Cell Biol*. 2002;3:906–918.
8. Resch-Genger U, Grabolle M, Cavaliere-Jaricot S, Nitschke R, Nann T. Quantum dots versus organic dyes as fluorescent labels. *Nat Methods*. 2008;5:763–775.
9. Reiss P, Protiere M, Li L. Core/shell semiconductor nanocrystals. *Small*. 2009;5:154–168.
10. Biju V, Itoh T, Ishikawa M. Delivering quantum dots to cells: bioconjugated quantum dots for targeted and nonspecific extracellular and intracellular imaging. *Chem Soc Rev*. 2010;39:3031–3056.
11. Zrazhevskiy P, Sena M, Gao X. Designing multifunctional quantum dots for bioimaging, detection, and drug delivery. *Chem Soc Rev*. 2010;39:4326–4354.
12. Medintz IL, Uyeda HT, Goldman ER, Mattoussi H. Quantum dot bioconjugates for imaging, labelling and sensing. *Nat Mater*. 2005;4:435–446.
13. Alivisatos AP, Gu WW, Larabell C. Quantum dots as cellular probes. *Annu Rev Biomed Eng*. 2005;7:55–76.
14. Michalet X. Quantum dots for live cells, *in vivo* imaging, and diagnostics. *Science*. 2005;307:538–544.
15. Gao XH, Chan WCW, Nie SM. Quantum-dot nanocrystals for ultrasensitive biological labeling and multicolor optical encoding. *J Biomed Opt*. 2002;7:532–537.
16. Liu WH, Greytak AB, Lee J, Wong CR, Park J, Marshall LF, Jiang W, Curtin PN, Ting AY, Nocera DG, Fukumura D, Jain RK, Bawendi MG. Compact biocompatible quantum dots via RAFT-mediated synthesis of imidazole-based random copolymer ligand. *J Am Chem Soc*. 2010;132:472–483.
17. Zhang BB, Xing D, Lin C, Guo FF, Zhao P, Wen XJ, Bao Z, Shi D. Improving colloidal properties of quantum dots with combined silica and polymer coatings for *in vitro* immuofluorenscence assay. *J Nanopart Res*. 2011;13:2407–2415.
18. Song S, Qin Y, He Y, Huang Q, Fan C, Chen H-Y. Functional nanoprobes for ultrasensitive detection of biomolecules. *Chem Soc Rev*. 2010;39:4234–4243.
19. Gao XH, Cui YY, Levenson RM, Chung LWK, Nie SM. In vivo cancer targeting and imaging with semiconductor quantum dots. *Nat Biotechnol*. 2004;22:969–976.
20. Sukhanova A, Devy M, Venteo L, Kaplan H, Artemyev M, Oleinikov V, Klinov D, Pluot M, Cohen JH, Nabiev I. Biocompatible fluorescent nanocrystals for immunolabeling of membrane proteins and cells. *Anal Biochem*. 2004;324:60–67.
21. Pellegrino T, Manna L, Kudera S, Liedl T, Koktysh D, Rogach AL, Keller S, Rädler J, Natile G, Parak WJ. Hydrophobic nanocrystals coated with an amphiphilic polymer shell: a general route to water soluble nanocrystals. *Nano Lett*. 2004;4:703–707.
22. Dubertret B, Skourides P, Norris DJ, Noireaux V, Brivanlou AH, Libchaber A. In vivo imaging of quantum dots encapsulated in phospholipid micelles. *Science*. 2002;298:1759–1762.
23. Pan J, Feng S-S. Targeting and imaging cancer cells by folate-decorated, quantum dots (QDs)-loaded nanoparticles of biodegradable polymers. *Biomaterials*. 2009;30:1176–1183.
24. Pan J, Wan D, Gong J. PEGylated liposome coated QDs/mesoporous silica core-shell nanoparticles for molecular imaging. *Chem Commun*. 2011;47:3442–3444.
25. Bentzen EL, Tomlinson ID, Mason J, Gresch P, Warnement MR, Wright D, Sanders-Bush E, Blakely R, Rosenthal SJ. Surface modification to reduce nonspecific binding of quantum dots in live cell assays. *Bioconjug Chem*. 2005;16:1488–1494.
26. Kairdolf BA, Mancini MC, Smith AM, Nie SM. Minimizing nonspecific cellular binding of quantum dots with hydroxyl-derivatizied surface coatings. *Anal Chem*. 2008;80:3029–3034.
27. Gref R, Domb A, Quellec P, Blunk T, Muller RH, Verbavatz JM, Langer R. The controlled intravenous delivery of drugs using peg-coated sterically stabilized nanospheres. *Adv Drug Deliv Rev*. 1995;16:215–33.
28. Simpson CA, Agrawal AC, Balinski A, Harkness KM, Cliffel DE. Short-chain PEG mixed monolayer protected gold clusters increase clearance and red blood cell counts. *ACS Nano*. 2011;5:3577–3584.
29. Bagwe RP, Hilliard LR, Tan WH. Surface modification of silica nanoparticles to reduce aggregation and nonspecific binding. *Langmuir*. 2006;22:4357–4362.
30. Nicolas J, Brambilla D, Carion O, Pons T, Maksimovic I, Larquet E, Le Droumaguet B, Andrieux K, Dubertret B, Couvreur P. Quantum dot-loaded PEGylated poly(alkyl cyanoacrylate) nanoparticles for *in vitro* and *in vivo* imaging. *Soft Matter*. 2011;7:6187–6193.
31. Song EQ, Zhang ZL, Luo QY, Lu W, Shi YB, Pang DW. Tumor cell targeting using folate-conjugated fluorescent quantum dots and receptor-mediated endocytosis. *Clin Chem*. 2009;55:955–963.
32. Daou TJ, Li L, Reiss P, Josserand V, Texier I. Effect of poly(ethylene glycol) length on the *in vivo* behavior of coated quantum dots. *Langmuir*. 2009;25:3040–3044.
33. Zhang ZP, Tan SW, Feng S-S. Vitamin E TPGS as a molecular biomaterial for drug delivery. *Biomaterials*. 2012;33:4889–4906.
34. Zhang Z, Mei L, Feng S-S. Vitamin E D-α-tocopheryl polyethylene glycol 1000 succinate-based nanomedicine. *Nanomedicine*. 2012;7:1645–1647.
35. Pan J, Feng S-S. Targeted delivery of paclitaxel using folate-decorated poly(lactide) - vitamin E TPGS nanoparticles. *Biomaterials*. 2008;29:2663–2672.
36. Pan J, Wang Y, Feng S-S. Formulation, characterization, and *in vitro* evaluation of quantum dots loaded in poly(lactide)-vitamin E TPGS nanoparticles for cellular and molecular imaging. *Biotechnol Bioeng*. 2008;101:622–633.
37. Mi Y, Liu Y, Feng S-S. Formulation of docetaxel by folic acid-conjugated d-α-tocopheryl polyethylene glycol succinate 2000 (Vitamin E TPGS2k) micelles for targeted and synergistic chemotherapy. *Biomaterials*. 2011;32:4058–4066.
38. Peng ZA, Peng XG. Formation of high-quality CdTe, CdSe, and CdS nanocrystals using CdO as precursor. *J Am Chem Soc*. 2001;123:183–184.
39. Ballou B, Lagerholm BC, Ernst LA, Bruchez MP, Waggoner AS. Noninvasive imaging of quantum dots in mice. *Bioconjug Chem*. 2004;15:79–86.
40. Chan WCW, Nie SM. Quantum dot bioconjugates for ultrasensitive nonisotopic detection. *Science*. 1998;281:2016–2018.
41. Fischer M, Georges J. Fluorescence quantum yield of rhodamine 6G in ethanol as a function of concentration using thermal lens spectrometry. *Chem Phys Lett*. 1996;260:115–118.

Manuscript received Sept. 5, 2013, and final revision received Jan. 20, 2014.